# 1 Theory of Elementary Particles

M. Bordone, S. Borowka, F. Buccioni, D. Buttazzo, X. Chen, L. Cieri, D. van Dyk, A. Gehrmann-De Ridder, T. Gehrmann, M. Grazzini, N. Greiner, A. Greljo, A. Ilnicka, C. Hanga, D. Hulme, A. Huss, D. Ivanov, M. Jaquier, D. Kara, G. Isidori, J. Lindert, P. Lowdon, N. A. Lo Presti, D. Marzocca, N. Moretti, J. Niehues, G. Oeztürk, M. Patra, A. Pattori, S. Pozzorini, D. Rathlev, H. Sargsyan, T, Schmidt, A. Signer, M. Schönherr, A. Visconti, M. Wiesemann, D. Wyler and M. Zoller

*in collaboration with:*
CERN, IMSc Chennai, Durham University, INFN Firenze, University of Buenos Aires, Freiburg University, Mainz University, INFN Genova, INFN Milano, University of Louvain, MPI Munich, INFN Padova, Peking University, Oxford University, INFN Roma, SLAC, ETH Zürich, DESY Hamburg, TU Dresden, TU Münich

The particle theory group at the Physik-Institut works on a broad spectrum of research projects related to the interpretation of data from high energy particle colliders. These cover precision calculations of benchmark observables, simulation of full collider events, identification of optimal observables for searches and measurements, physics beyond the Standard Model (SM), as well as developments of calculational techniques. We summarize some highlights of last year's research below.

### 1.1 Vector boson pair production at NNLO

The production of vector-boson pairs is a relevant process for physics studies within and beyond the SM. First of all, this process can be used to measure the vector boson trilinear couplings. Any deviation from the coupling structure predicted by $SU(2) \otimes U(1)$ gauge invariance would be a signal of new physics. The Tevatron collaborations have measured cross sections for vector-boson pair production at invariant masses larger than those probed at LEP2, setting limits on the corresponding anomalous couplings, and the LHC experiments are now continuing this research program. Vector boson pairs provide also an important background for new physics searches.

Up to a few years ago, the status of theoretical predictions for vector-boson pair production was essentially limited to next-to-leading order (NLO) in QCD perturbation theory. The bottleneck was essentially the knowledge of the relevant two-loop amplitudes. Recently, a major step forward has been carried out, with the evaluation of all the two-loop planar and non planar master integrals relevant for the production of off-shell vector boson pairs, and the calculation of the corresponding helicity amplitudes has been completed.

Even having all the relevant amplitudes, the computation of the next-to-next-to-leading order (NNLO) corrections is still a non-trivial task, due to the presence of infrared (IR) singularities at intermediate stages of the calculation, and numerical techniques cannot be straightforwardly applied. To handle and cancel these singularities at NNLO the $q_T$ subtraction formalism [6] is particularly suitable, since it is fully developed to work in the hadronic production of heavy colourless final states.



In the following we present theoretical predictions [1] for the case of $Z\gamma$ and $W\gamma$ production at the LHC and compare them with the ATLAS data from Ref. [2]. The required tree-level and one-loop amplitudes were obtained with the OpenLoops [3] generator, which employs the Denner-Dittmaier algorithm for the numerical evaluation of one-loop integrals and implements a fast numerical recursion for the calculation of NLO scattering amplitudes within the SM. The two loop amplitudes are taken from [4].

For the electroweak couplings we use the so-called $G_\mu$ scheme, where the input parameters are $G_F$, $m_W$, $m_Z$. In particular we use the values $G_F = 1.16639 \times 10^{-5}$ GeV$^{-2}$, $m_W = 80.399$ GeV, $m_Z = 91.1876$ GeV, $\Gamma_Z = 2.4952$ GeV and $\Gamma_W = 2.1054$ GeV. We set the CKM matrix to unity. We use the MMHT 2014 [5] sets of parton distribution functions (PDFs), with densities and $\alpha_S$ evaluated at each corresponding order (i.e., we use $(n+1)$-loop $\alpha_S$ at N$^n$LO, with $n = 0, 1, 2$), and we consider $N_f = 5$ massless quarks/antiquarks and gluons in the initial state. The default renormalization ($\mu_R$) and factorization ($\mu_F$) scales are set to $\mu_R = \mu_F = \mu_0 \equiv \sqrt{m_V^2 + (p_T^\gamma)^2}$, where $m_V$ is the mass of the vector boson and $p_T^\gamma$ the transverse momentum of the photon. Scale uncertainties are estimated by varying $\mu_F$ and $\mu_R$ independently in the range $0.5\mu_0$ and $2\mu_0$.

The present formulation of the $q_T$ subtraction formalism [6] is limited to the production of colourless sys-

TAB. 1.1 –
Results on fiducial cross sections to the ATLAS 7 TeV analyses on $pp \to \ell\nu\gamma$, $pp \to \ell\ell\gamma$, and $pp \to \nu\nu\gamma$. Event-selection criteria are detailed in Tables 1,4,6 of Ref. [1].

| | $p_{\mathrm{T,cut}}^{\gamma}$ [GeV] | $N_{\mathrm{jet}}$ | $\sigma_{\mathrm{LO}}$ [pb] | $\sigma_{\mathrm{NLO}}$ [pb] | $\sigma_{\mathrm{NNLO}}$ [pb] | $\sigma_{\mathrm{ATLAS}}$ [pb] | $\frac{\sigma_{\mathrm{NLO}}}{\sigma_{\mathrm{LO}}}$ | $\frac{\sigma_{\mathrm{NNLO}}}{\sigma_{\mathrm{NLO}}}$ |
|---|---|---|---|---|---|---|---|---|
| $pp \to W\gamma \to \ell\nu\gamma + X$ | 15 | $\geq 0$ | $0.8726\,^{+6.8\%}_{-8.1\%}$ | $2.058\,^{+6.8\%}_{-6.8\%}$ | $2.453\,^{+4.1\%}_{-4.1\%}$ | 2.77 $\pm 0.03$ (stat) $\pm 0.33$ (syst) $\pm 0.14$ (lumi) | 2.36 | 1.19 |
| @ $\sqrt{s} = 7\,\mathrm{TeV}$ | 15 | $= 0$ | $0.8726\,^{+6.8\%}_{-8.1\%}$ | $1.395\,^{+5.2\%}_{-5.8\%}$ | $1.493\,^{+1.7\%}_{-2.7\%}$ | 1.76 $\pm 0.03$ (stat) $\pm 0.21$ (syst) $\pm 0.08$ (lumi) | 1.60 | 1.07 |
| | 40 | $\geq 0$ | $0.1158\,^{+2.6\%}_{-3.7\%}$ | $0.3959\,^{+9.0\%}_{-7.3\%}$ | $0.4971\,^{+5.3\%}_{-4.7\%}$ | | 3.42 | 1.26 |
| $pp \to Z\gamma \to \ell^+\ell^-\gamma + X$ | 15 | $\geq 0$ | $0.8149\,^{+8.0\%}_{-9.3\%}$ | $1.222\,^{+4.2\%}_{-5.3\%}$ | $1.320\,^{+1.3\%}_{-2.3\%}$ | 1.31 $\pm 0.02$ (stat) $\pm 0.11$ (syst) $\pm 0.05$ (lumi) | 1.50 | 1.08 |
| @ $\sqrt{s} = 7\,\mathrm{TeV}$ | 15 | $= 0$ | $0.8149\,^{+8.0\%}_{-9.3\%}$ | $1.031\,^{+2.7\%}_{-4.3\%}$ | $1.059\,^{+0.7\%}_{-1.4\%}$ | 1.05 $\pm 0.02$ (stat) $\pm 0.10$ (syst) $\pm 0.04$ (lumi) | 1.27 | 1.03 |
| | 40 | $\geq 0$ | $0.0736\,^{+3.4\%}_{-4.5\%}$ | $0.1320\,^{+4.2\%}_{-4.0\%}$ | $0.1543\,^{+3.1\%}_{-2.8\%}$ | | 1.79 | 1.17 |
| $pp \to Z\gamma \to \nu\bar{\nu}\gamma + X$ | 100 | $\geq 0$ | $0.0788\,^{+0.3\%}_{-0.9\%}$ | $0.1237\,^{+4.1\%}_{-3.1\%}$ | $0.1380\,^{+2.5\%}_{-2.3\%}$ | 0.133 $\pm 0.013$ (stat) $\pm 0.020$ (syst) $\pm 0.005$ (lumi) | 1.57 | 1.12 |
| @ $\sqrt{s} = 7\,\mathrm{TeV}$ | 100 | $= 0$ | $0.0788\,^{+0.3\%}_{-0.9\%}$ | $0.0881\,^{+1.2\%}_{-1.3\%}$ | $0.0866\,^{+1.0\%}_{-0.9\%}$ | 0.116 $\pm 0.010$ (stat) $\pm 0.013$ (syst) $\pm 0.004$ (lumi) | 1.12 | 0.98 |



tems $F$ and, hence, it does not allow us to deal with the parton fragmentation subprocesses. Therefore, we consider only direct photons, and we rely on the smooth cone isolation criterion. Considering a cone of radius $r = \sqrt{(\Delta\eta)^2 + (\Delta\phi)^2}$ around the photon, we require that the total amount of hadronic (partonic) transverse energy $E_T$ inside the cone is smaller than $E_T^{\mathrm{max}}(r)$,

$$E_T^{\mathrm{max}}(r) \equiv \epsilon_\gamma\, p_T^\gamma \left(\frac{1-\cos r}{1-\cos R}\right)^n ;$$

the isolation criterion $E_T < E_T^{\mathrm{max}}(r)$ has to be fulfilled for all cones with $r \leq R$. All results presented here are obtained with $\epsilon_\gamma = 0.5$, $n = 1$ and $R = 0.4$.

Jets are reconstructed with the anti-$k_T$ algorithm with radius parameter $D = 0.4$, and a jet must have a transverse momentum $p_T^{\mathrm{jet}} > 30$ GeV and pseudorapidity $|\eta^{\mathrm{jet}}| < 4.4$.

We compare our predictions to the ATLAS results for $W\gamma$ and $Z\gamma$ at a centre of mass energy of 7 TeV [2]. Experimental results and theoretical predictions on fiducial cross sections are collected in Table 1.1 for the different channels, with and without a veto against jets. The precise kinematic cuts to define these fiducial cross sections are detailed in Tables 1, 4, 6 of Ref. [1], and are not repeated here.

The predicted inclusive $W\gamma$ cross sections ($W^+\gamma$ and $W^-\gamma$ are always summed over) with the soft $p_T^\gamma$ cut of 15 GeV are quite large: the NLO $K$ factor is +136%, and the NNLO corrections increase the NLO results by +19%. The measurement of the inclusive cross section by ATLAS shows a $2\sigma$ excess with respect to the NLO prediction, which is reduced to well below $1\sigma$ when including the NNLO corrections. The impact of QCD corrections at NLO and NNLO is reduced to 60% and 7%, respectively, when a jet veto is applied ($N_{\mathrm{jet}} = 0$). Such an effect is expected and apparently leads to a more stable perturbative prediction, but also to the possible need of more conservative procedures to estimate perturbative uncertainties. In the exclusive case, the excess of the measured fiducial cross sections over the theoretical prediction is reduced from $1.6\sigma$ to $1.2\sigma$ when going from NLO to NNLO. We note that the scale variations at NLO significantly underestimate the impact of the NNLO corrections, in particular in the inclusive case.

The predicted $Z\gamma$ cross sections in the visible $Z$ decay mode with the soft $p_T^\gamma$ cut of 15 GeV get corrected by +50% (+27%) at NLO and by +8% (+3%) at NNLO in the inclusive (exclusive) case, respectively. Both the NLO and NNLO predictions are in agreement with the experimental results, and the NNLO corrections improve the agreement, especially in the inclusive case.

It is obvious that the $W\gamma$ process features much larger radiative effects with respect to the $Z\gamma$ process, which should be contrasted to what happens in the case of inclusive $W$ and $Z$ boson production, where QCD radiative

corrections are essentially identical. It is thus the emission of the additional photon that breaks the similarity between the charged-current and the neutral-current processes. By studying the LO contributions to the $Z\gamma$ and $W\gamma$ cross sections it turns out that the additional Feynman diagram in which the photon is radiated off the $W$ boson gives rise to a *radiation zero* [7], which does not exist in $Z\gamma$ production. This exact zero, present in the on-shell partonic $W\gamma$ tree-level amplitude at $\cos\theta^* = 1/3$, where $\theta^*$ is the scattering angle in the centre-of-mass frame, gets diluted by the convolution with the parton densities and by off-shell effects, but it is responsible for the suppression of the Born level $W\gamma$ cross section with respect to $Z\gamma$. Real radiation appearing beyond LO breaks the radiation zero, and thus the relative impact of higher-order corrections is significantly increased.

Besides the cross section in the fiducial region, ATLAS has also provided the measured cross sections differential in the photon transverse momentum. A comparison of the resulting distributions with our theoretical NLO and NNLO predictions is shown in Fig. 1.1 for the processes $pp(\to W\gamma) \to \ell\nu\gamma$ (upper plots) and $pp(\to Z\gamma) \to \ell^+\ell^-\gamma$ (lower plots), both for the inclusive (left plots) and the exclusive (right plots) case. In general, the inclusion of NNLO corrections significantly improves the agreement between data and theory. The improvement is particularly important in the inclusive $W\gamma$ case, and less pronounced for $Z\gamma$ and for the exclusive predictions, where the overall size of NNLO corrections is significantly smaller.

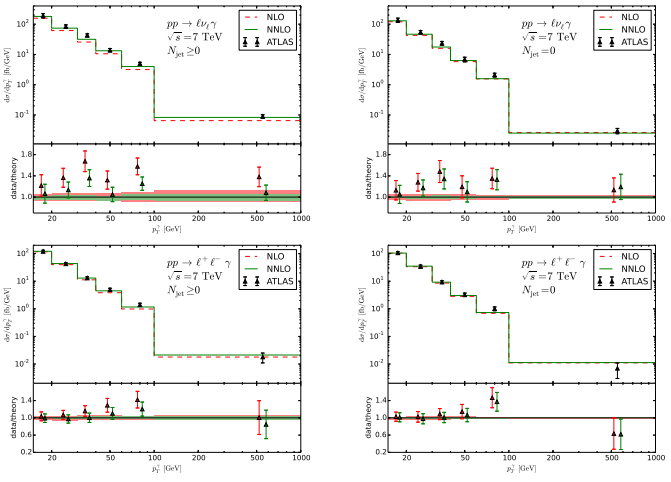


FIG. 1.1 – Photon transverse momentum distribution for the processes $pp(\to W\gamma) \to \ell\nu\gamma$ (upper plots) and $pp(\to Z\gamma) \to \ell^+\ell^-\gamma$ (lower plots) in the inclusive (left) and exclusive case (right) at NLO (red, dashed) and NNLO (green, solid) compared to ATLAS data. In the upper panel, only experimental uncertainties are shown. The lower panel shows the data/theory ratio for both theory predictions, and the bands indicate theoretical uncertainty estimates from scale variations.

When switching to a harder cut of 40 GeV on $p_T^\gamma$, Table 1.1 shows significantly increased corrections of $+242\%$ and $+79\%$ at NLO and of $+26\%$ and $+19\%$ at NNLO for the processes $pp(\to W\gamma) \to \ell\nu\gamma$ and $pp(\to Z\gamma) \to \ell^+\ell^-\gamma$, respectively.

The predicted fiducial cross sections for $pp \to \nu\bar{\nu}\gamma$ in the ATLAS setup at 7 TeV [2] are presented in Table 1.1, summed over three neutrino channels, and show relative corrections of $+57\%$ ($+12\%$) at NLO and $+12\%$ ($-2\%$) at NNLO in the inclusive (exclusive) case. The inclusive NNLO prediction is in good agreement with the cross section measured by ATLAS. In the exclusive case, $N_{\text{jet}} = 0$, the NNLO corrections are very small, with most likely underestimated scale uncertainties at the 1% level, and we observe quite a significant discrepancy with respect to the ATLAS measurement. This can be understood by hadronization corrections, which are expected to be small for all the other discussed processes, but lead to sizeable effects in $\nu\bar{\nu}\gamma$, particularly for $N_{\text{jet}} = 0$.


[1] M. Grazzini, S. Kallweit and D. Rathlev, JHEP **1507** (2015) 085.

[2] G. Aad *et al.* [ATLAS Collaboration], Phys. Rev. D **87** (2013) 11, 112003. Erratum: [Phys. Rev. D **91** (2015) no.11, 119901].

[3] F. Cascioli, P. Maierhofer and S. Pozzorini, Phys. Rev. Lett. **108** (2012) 111601.

[4] T. Gehrmann and L. Tancredi, JHEP **1202** (2012) 004.

[5] L. A. Harland-Lang, A. D. Martin, P. Motylinski and R. S. Thorne, Eur. Phys. J. C **75** (2015) no.5, 204.

[6] S. Catani and M. Grazzini, Phys. Rev. Lett. **98** (2007) 222002.

[7] K. O. Mikaelian, M. A. Samuel and D. Sahdev, Phys. Rev. Lett. **43** (1979) 746.




## 1.2 Two-loop five-point functions in QCD

The precise theoretical description of scattering reactions of elementary particles relies on the perturbation theory expansion of the scattering amplitudes describing the process under consideration. In this expansion, higher perturbative orders correspond to more and more virtual particle loops. At present, one-loop corrections can be computed to scattering amplitudes of arbitrary multiplicity, while two-loop corrections are known only for selected two-to-one annihilation or two-to-two scattering processes.

For many experimental observables at higher multiplicity, a substantial increase in statistical precision can

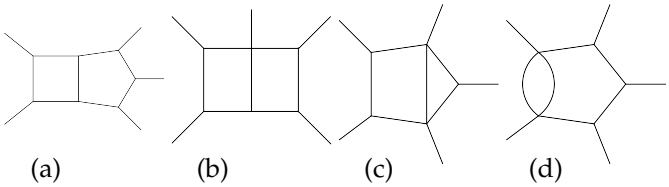


FIG. 1.2 – Genuine five-point planar two-loop integrals.

be expected from the CERN LHC in the near future. Perturbative predictions beyond one loop will be in demand for many precision applications of these data, for example in improved extractions of SM parameters or in search for indirect signatures of new high-scale physics in precision observables. Progress on multi-loop corrections to high-multiplicity amplitudes requires significant advances in two directions: the reduction of the large number of multi-loop Feynman integrals that appear in the amplitude to a small set of so-called master integrals, and the evaluation of the master integrals themselves.

During the last year, we analytically computed for the first time the full set of planar master integrals relevant to massless two-loop five-point scattering [8]. The calculation was made possible by technical advances in the calculation of multi-loop Feynman integrals.

The type of master integrals that appear in a given process depends only on the external kinematics, and on possible internal propagator masses. All two-loop five-parton amplitudes relate to a common set of master integrals: massless on-shell five-point functions at two loops. These can be further classified into genuine five-point functions, four-point functions with one off-shell leg, three-point functions with up to two off-shell legs and off-shell two-point functions. Up to the four-point level, these functions appeared in the context of the derivation of the two-loop amplitude for $\gamma^\star \to 3$ jets and were already computed long ago. For the genuine five-point functions, we find in total 25 new integrals (10 planar and 15 non-planar). The planar integrals can be given in terms of four integral topologies, displayed in Figure 1.2. There are 3, 3, 2, and 2 master integrals for topologies (a), (b), (c), and (d), respectively.

To compute the integrals, we derive differential equations for them in the Mandelstam invariants. The system of differential equations is then brought into a canonical form by means of a transformation of the basis of master integrals to integrals having unit leading singularities. The full set of master integrals can be obtained by direct integration of the differential equations, order-by-order in $\epsilon$, in terms of Chen iterated integrals. Massless scattering is naturally parametrized using momentum twistor variables that solve both the on-shell as well as the momentum conservation constraints. When expressed in terms of these variables, the Chen iterated integrals degenerate to multiple poly-logarithms, for which efficient and precise numerical representations exist.

As a first application of our newly computed integrals, we consider the all-plus helicity five-gluon amplitude at leading color. Since this amplitude vanishes at tree level, it is finite at the one-loop level. Its reduction to master integrals has been derived earlier in the literature. By inserting our expressions for these integrals, we arrive at a relatively simple expression for its finite remainder

$$F_5^{(2)} = \frac{5\pi^2}{12} F_5^{(1)} + \sum_{i=0}^{4} \sigma^i \left\{ \frac{v_5 \mathrm{tr}\left[(1-\gamma_5) \not{p}_4 \not{p}_5 \not{p}_1 \not{p}_2\right]}{(v_2+v_3-v_5)} I_{23,5} + \frac{1}{6} \frac{\mathrm{tr}\left[(1+\gamma_5) \not{p}_4 \not{p}_5 \not{p}_1 \not{p}_2\right]^2}{v_1 v_4} + \frac{10}{3} v_1 v_2 + \frac{2}{3} v_1 v_3 \right\},$$

where the $v_i$ are Mandelstam invariants of adjacent moments and $\sigma^i$ cyclically shifts all indices by $i$, and where

$$I_{23,5} = \zeta_2 + \mathrm{Li}_2\left[\frac{(v_5-v_2)(v_5-v_3)}{v_2 v_3}\right] - \mathrm{Li}_2\left[\frac{v_5-v_3}{v_2}\right] - \mathrm{Li}_2\left[\frac{v_5-v_2}{v_3}\right].$$

The simplicity of our result for the all-plus amplitude in QCD is reminiscent of similar results for multi-leg amplitudes in supersymmetric theories. It opens up new possibilities for multi-loop calculations of high-multiplicity processes. Extensions to non-planar integrals and to the full set helicities for five-parton two-loop amplitudes are currently under way.

[8] T. Gehrmann, J. M. Henn and N. A. Lo Presti, Phys. Rev. Lett. **116** (2016) 062001.

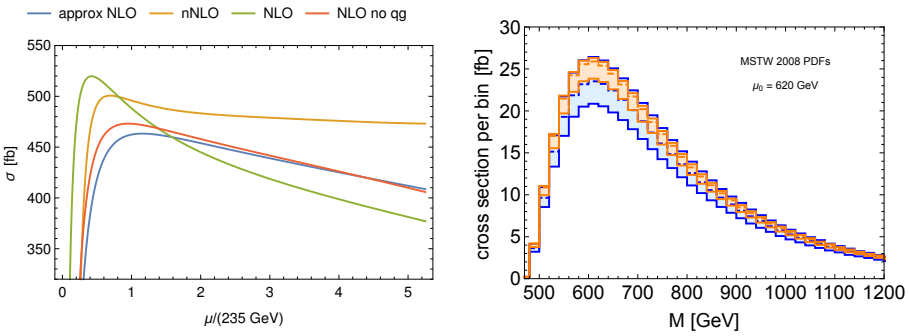


FIG. 1.3 – Scale dependence of various approximations to the total cross section for a Higgs and a top pair (left panel) and invariant mass distribution of the $t\bar{t}H$ system (right panel) for the 13 TeV LHC. The approximate NNLO prediction (orange band), denoted by nNLO, is compared to the NLO prediction (blue band).

## 1.3 Associated production of a Higgs and a top pair beyond NLO

According to the SM the coupling of a Higgs boson to a fermion is proportional to the mass of the fermion. Hence, the coupling between the Higgs and the top quark, the heaviest known elementary fermion, provides a stringent test of our understanding on how elementary particles obtain their mass. Information on this coupling can be obtained by studying the associated production of a top pair and a Higgs boson.

Typically, calculations at NLO in perturbation theory lead to uncertainties of about $20-30\%$ for this process. While a full NNLO calculation is currently technically not feasible, not even for the total cross section, in Ref. [9] results that go beyond a NLO calculation have been presented for the total cross section and for differential distributions. Approximate NNLO (nNLO) corrections have been computed by applying renormalization-group techniques. This allows to determine those NNLO terms that are enhanced by logarithms. Near threshold, these terms are expected to be dominant and give a reliable estimate of the full NNLO correction.

As an illustration in the left panel of Figure 1.3 the improvement on the scale dependence for the total cross section is shown when going from NLO (green curve) to nNLO (orange). To validate the method, a comparison between the NLO result (red) and approximate NLO result (blue) is also shown for those channels that are included in the approximation ($q\bar{q}$ and $gg$ initial states). The neglect of the remaining subleading channels ($qg$ and $\bar{q}g$ initial states) is compensated for by associating an additional uncertainty due to a conservative estimate of subleading terms.

The result of applying this method to the distribution of the invariant mass of the top pair and the Higgs is shown in the right panel of Figure 1.3. The uncertainty at NLO (blue band) is substantially reduced when going to nNLO (orange band). Results for other distributions also including cuts can be obtained similarly.

[9] A. Broggio, A. Ferroglia, B. D. Pecjak, A. Signer and L. L. Yang, JHEP **1603** (2016) 124.

## 1.4 Physics beyond the Standard Model

### 1.4.1 Pseudo Observables in Higgs physics

Characterizing the properties of the Higgs boson with high precision and minimal theoretical bias is of great importance to investigate the nature of physics beyond the SM. This is the purpose of the so-called Higgs *Pseudo Observables* (PO) approach, developed by our research group in 2014. The Higgs PO are a set of quantities that are well defined from the quantum field theory point of view, that are experimentally accessible, and that allow to characterize possible deviations from the SM in great generality. In 2014 we have classified all the PO relevant to describe Higgs decays. In 2015 we have further developed the approach along three main directions: i) we have identified the PO necessary to describe also Higgs production processes [10]; ii) we have analyzed the effect of electroweak bounds on the PO under the hypothesis that the $h(125)$ particle is the massive excitation of a pure $SU(2)_L$ doublet [11, 12]; iii) we have investigated the effect of NLO radiative corrections in the description of Higgs decays in generic extensions of the SM [13].

In Fig. 1.4 we show the prediction of the $h \to 2e2\mu$ decay spectrum obtained using the PO decomposition (with PO set to their SM values), with and without the inclusion of radiative corrections [13]. The spectrum thus obtained is compared with the complete NLO SM result obtained using the numerical code Prophecy4f. The excellent agreement of the two results is a demonstration of the capability of the PO approach to recover the best up-to-date predictions in the SM case while, at the same, allowing a general description of physics beyond the SM.

One of the most difficult measurement of Higgs couplings at the LHC is the determination of the charm Yukawa couplings. In Ref. [14] we have proposed a new method to determine this coupling via the Higgs production in association with a charm-tagged jet: $\sigma(pp \to hc)$. As a first estimate, we have found that at the LHC with 3000 fb$^{-1}$ it should be possible to derive a constraint of order one, relative to the SM value, for the charm Yukawa coupling.

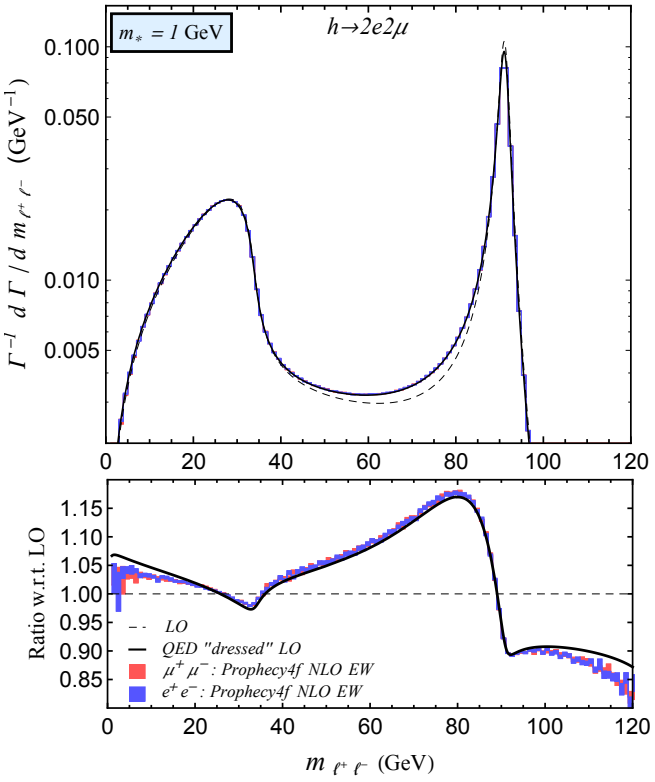


FIG. 1.4 – Dilepton invariant mass spectrum in the SM for the $h \to 2e2\mu$ decay (full line: PO decomposition "dressed" with QED corrections; red and blue bands: complete NLO result from Prophecy4f).

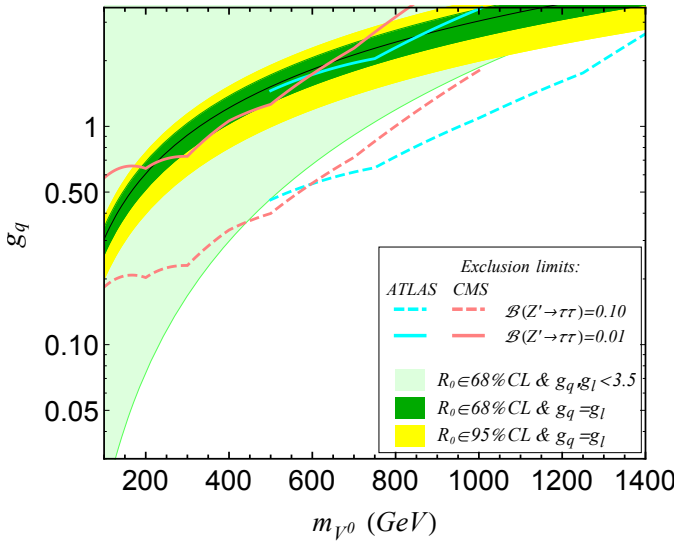


FIG. 1.5 – Mass and coupling of the vector mediator proposed in Ref. [15] to explain the anomalies observed in $B$ decays. The preferred region from the low-energy fit is the green (yellow) band. The dotted lines denote the exclusion limits (below the curve) from direct searches of massive vectors decaying into $\tau^+\tau^-$ pairs at the LHC, assuming different branching ratios ($\mathcal{B}$). The minimal model predicts $\mathcal{B} = 0.1$, but smaller values can be obtained in extended models.



### 1.4.2 Anomalies in $B$ decays

In view of recent experimental indications of violations of Lepton Flavor Universality (LFU) in $B$ decays, we have analyzed the constraints and implications of LFU interactions, both using an effective theory approach, and employing explicit dynamical models [15, 16].

In Ref. [15] we have shown that a simple dynamical model based on a $SU(2)_L$ triplet of massive vector bosons, coupled predominantly to third generation fermions (both quarks and leptons), can significantly improve the description of present data. In particular, the model decreases the tension between data and SM predictions concerning: i) the breaking of $\tau$–$\mu$ universality in $B \to D^{(*)}\ell\nu$ decays; ii) the breaking of $\mu$–$e$ universality in $B \to K\ell^+\ell^-$ decays. Indirectly, the model might also decrease the discrepancy between exclusive and inclusive determinations of $|V_{cb}|$ and $|V_{ub}|$. The minimal version of the model is in tension with ATLAS and CMS direct searches for the new massive vectors (decaying into $\tau^+\tau^-$ pairs), and shown in Fig. 1.5, but this tension can be decreased with additional non-standard degrees of freedom. Further predictions of the model both at low- and high-energies, in view of future high-statistics data, have also been discussed.

In Ref. [16] we have shown that an equally good explanation of present data can be obtained in the context of a weakly broken $U(2)^5$ flavor symmetry (similarly to the case discussed above), but with lepto-quark vector mediators rather than colorless vector fields.

### 1.4.3 The di-photon excess and other aspects of physics beyond the SM

At the end of 2015 the ATLAS and CMS experiments, after the analysis of the first 13 TeV data, have reported evidences of an excess in the $pp \to 2\gamma$ inclusive distribution for $m_{2\gamma} \approx 750$ GeV. While the evidence of this excess is not yet statistically very large, it is interesting to ask the question if this anomaly can be interpreted as the first direct hint of physics beyond the SM.

A first analysis along this line has been presented in Ref. [17], where it has been shown that interpretation of the signal as a new scalar resonance produced in gluon fusion and decaying to photons is consistent with all relevant exclusion bounds from the 8 TeV LHC run. A simple phenomenological framework to parametrize the properties of the new resonance has also been provided. Using this tool it has been shown in a model-independent way that, if the scalar is produced in gluon fusion, additional new colored and charged particles are re-

quired. Some more specific interpretations in various concrete setups, such as a singlet (pseudo-) scalar, composite Higgs, and the MSSM have also beed discussed.

In recent years there has been considerable interest in the problem of the stability of the SM ground state, in the limit where no new physics appear up to very high energy scales. In Ref. [18] we have reviewed the formalism by which the tunneling probability of an unstable ground state can be computed in quantum field theory, with special reference to the Standard Model of electroweak interactions. We have described in some detail the approximations implicitly adopted in such calculations, devoting particular attention to the role of scale invariance. By means of this analysis we have shown that new interactions characterized by a new energy scale, close to the Planck mass, do not invalidate the main conclusions about the stability of the Standard Model ground state derived in absence of such terms (contrary to recent claims of the opposite present in the recent literature). The scope of these analyses is answering the following well-defined physical question: *Does the extrapolation of the SM up to the Planck scale necessarily imply the existence of NP below such a scale?* According to the present experimental values of $m_h$ and $m_t$, we can state that the answer to this question is *no*.


[10] A. Greljo, G. Isidori, J. M. Lindert and D. Marzocca, Eur. Phys. J. C **76** (2016) 158.

[11] M. Gonzalez-Alonso, A. Greljo, G. Isidori and D. Marzocca, Eur. Phys. J. C **75** (2015) 341.

[12] A. Falkowski, M. Gonzalez-Alonso, A. Greljo and D. Marzocca, Phys. Rev. Lett. **116** (2016) 011801.

[13] M. Bordone, A. Greljo, G. Isidori, D. Marzocca and A. Pattori, Eur. Phys. J. C **75** (2015) 385.

[14] I. Brivio, F. Goertz and G. Isidori, Phys. Rev. Lett. **115** (2015) 211801.

[15] A. Greljo, G. Isidori and D. Marzocca, JHEP **1507** (2015) 142.

[16] R. Barbieri, G. Isidori, A. Pattori and F. Senia, Eur. Phys. J. C **76** (2016) 67.

[17] D. Buttazzo, A. Greljo and D. Marzocca, Eur. Phys. J. C **76** (2016) 116.

[18] L. Di Luzio, G. Isidori and G. Ridolfi, Phys. Lett. B **753** (2016) 150.